Hidden topological order in the heavy fermion metal URu_2Si_2

Tanmoy Das[1,2]
[1]*Theoretical Division, Los Alamos National Laboratory, Los Alamos, NM, 87545, USA.*
[2]*Physics Department, Northeastern University, Boston, MA, 02115, USA.*
(Dated: February 6, 2012)

We present a novel order parameter for the hidden order state of URu_2Si_2. We show via *ab-initio* calculation and low-energy effective tight-binding model that an incommensurate Fermi surface nesting in the partially-filled f-states renders a spin-orbit coupling density wave in the hidden-order state. An observable quantity for this order parameter is the polarized total angular momentum Δm_J=$\pm$2, consistent with neutron scattering measurements. The staggered spin-orbit coupling breaks spontaneous rotational symmetry, while time-reversal symmetry remains intact, and thus can be destroyed by magnetic field even at $T = 0$ K. We compute the topological properties to show that the hidden-order gap opening is associated with a trivial to non-trivial topological phase transition. The results suggest that the hidden order phase transition can inherit a novel 'topological quantum critical point', encoding both a topological and a second-order phase transition as a function of magnetic field.

PACS numbers: 71.27.+a,03.65.Vf,74.40.Kb,75.25.Dk

Most states or phases of matter can be described by local order parameters and the associated broken symmetries in the spin, charge, orbital or momentum channel. However, recent discoveries of quantum Hall states,[1] and topological insulators[2, 3] have revamped this conventional view. It has been realized[1–4] that systems with combined time-reversal ($\mathcal{TR}$) symmetry and large spin-orbit coupling (SOC) can host new states of matter which are distinguished by topological quantum numbers of the bulk band structure rather than spontaneously broken symmetries. Subsequently, more such distinct phases have been proposed in the family of topological Mott insulators,[5] topological Kondo insulators,[6] topological antiferromagnetic insulators,[7]. In these cases, the combined many-body physics and $\mathcal{TR}$ symmetry governs topologically protected quantum phases. Encouraged by these breakthrough developments, we search for analogous exotic phases in the heavy fermion metal URu_2Si_2, whose low-energy f states accommodate $\mathcal{TR}$ and strong SOC. This compound also naturally hosts diverse quantum mechanical phases including Kondo physics, large moment antiferromagnetism (LMAF), mysterious 'hidden-order' (HO) state, and superconductivity.[8].

In URu_2Si_2 the screening of f-electrons due to the Kondo effect begins at relatively high temperatures, ushering the system into a heavy fermion metal at low-temperature.[9] Below T_h=17.5 K, it enters into the HO state via a second-order phase transition characterized by sharp discontinuities in numerous bulk properties.[10–13] The accompanying gap is opened both in the electronic structure[9, 14–16] as well as in the magnetic excitation spectrum,[17] suggesting the formation of an itinerant magnetic order at this temperature. However, the associated tiny moment ($m_0 \approx 0.03\mu_B$) cannot account for the large (about 24%) entropy release[18] and other sharp thermodynamic[10, 11] and transport anomalies[12, 13] during the transition. Furthermore, very different evolutions of the HO parameter and the secondary magnetic moment as a function of both magnetic field[19, 20] and pressure[21, 22] rules out a magnetic origin of the HO phase in this system. Any compelling evidence for other charge, orbital or structural ordering has also not been obtained.[23] From theoretical point of view, there have been numerous proposals for the microscopic origin of HO parameter as listed together in Ref. 24. More recent efforts to understand the observed in-plane anisotropy include spin nematic order,[34] modulated spin liquid,[35] j-j fluctuations.[36] However, a general consensus of the nature of the HO state has not yet been attained.[8]

Formulating the correct model for the HO state primarily hinges on identifying which electronic symmetries (if any) are broken, what the identity of any associated order parameter might be, and which microscopic electronic degrees of freedom are active. A recent torque measurement on high quality single crystal sample reveals that the four-fold rotational symmetry of the crystal becomes spontaneously broken[23] at the onset of the HO state. This result has received further support from several momentum-resolved spectroscopic data where the presence of a longitudinal incommensurate FS 'hot-spot' at $\boldsymbol{Q}_h = (1 \pm 0.4, 0, 0)$ has been unambiguously established.[14, 16, 18, 37] [Previous first-principle calculation has demonstrated that an accompanying commensurate nesting at $\boldsymbol{Q}_2 = (1, 0, 0)$ might be responsible for the LMAF phase,[38] which is separated from the HO state via a first order phase transition.[8, 19–22]. As one cannot have two phases of same broken symmetry, but separated by a phase boundary, we expect that LMAF and HO phases are different.] Based on these observations, a consistent picture emerges that the HO state originates from a Fermi surface (FS) instability at nesting $\boldsymbol{Q}_h$. This unidirectional 'hot-spot' breaks the four-fold tetragonal symmetry of URu_2Si_2 to open a FS gap. In general, the order parameter that emerges due to a broken symmetry relies incipiently on the good quantum number of the 'parent' or non-interacting Hamiltonian. In case of URu_2Si_2, spin and orbital are not the good quantum numbers[39], rather the presence of the SOC renders the total angular momentum to become the good quantum number. The 'parent' Hamiltonian also accommodate other symme-

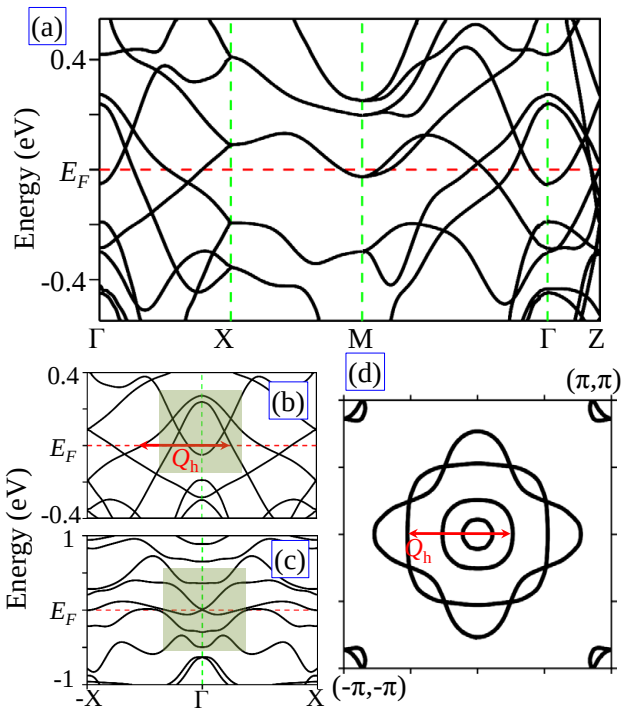

FIG. 1. (a) Computed non-interacting energy dispersions of URu_2Si_2, using Wien2K software, are presented along Γ(0,0,0), X(π,0,0), M(π,π,0), and Z(0,0,π) directions.[40, 41] The band structure is consistent with the previous full potential local orbitals (FPLO) and full potential linearized augmented plane wave (FPLAPW) calculations in the paramagnetic state.[38] The low-energy dispersions along Γ-X is expanded in (b) and contrasted with the same but without the SOC in (c). The FS in the $k_z = 0$ plane is shown in (d). The red arrow dictates the FS 'hot-spot' that emerges after including SOC.

tries coming from its crystal, wavefunction properties which we desire to incorporate to formulate the HO parameter.

Ab-initio band structure:-In order to find out the symmetry properties of the low-lying states, we begin with investigating the *ab-initio* 'parent' band dispersion and the FS of URu_2Si_2[40, 41] in Fig. 1. To closely examine how a longitudinal FS 'hot-spot' originates due to the turning on of SOC, we compare the band structure along the Γ-X direction near the Fermi level (E_F) for calculations with and without SOC (Figs. 1(b) and 1(c), respectively). The electronic structure in the vicinity of E_F ($\pm$0.2eV) is dominated by the $5f$ states of U atom in the entire Brillouin zone.[14–16, 37, 38, 42] Owing to the SOC and the tetragonal symmetry, the $5f$ states split into the octet J=$\frac{7}{2}$ (Γ_8) states and the sextet J=$\frac{5}{2}$ (Γ_6) states.[43] URu_2Si_2 follows a typical band progression in which the Γ_8 bands are pushed upward to the empty states while the Γ_6 states drop to the vicinity of the Fermi level. The corresponding FS in Fig. 1(d) reveals that an even number of anti-crossing features occurs precisely at the intersection between two oppositely dispersing conducting sheets. Unlike in topological insulators,[3, 4] the departure of the band crossing points from the $\mathcal{TR}$-invariant momenta here precludes the opening of an inverted band gap at the crossings,[2] and Dirac-cones crop up with Kramer's degeneracy in the bulk states. Therefore, URu_2Si_2 is an intrinsically trivial topological metal above the HO transition temperature.

The SOC introduces two prominent FS nestings at $Q_2 = (1, 0, 0)$ and at $Q_h = (1 \pm 0.4, 0, 0)$.[44] The commensurate nesting Q_2 occurs between intra-orbitals. Therefore, if this instability induces a gap opening, it has to be in the spin-channel, which is prohibited by $\mathcal{TR}$ symmetry and strong SOC. We argue (see Ref. 45 for details), in accordance with an earlier calculation,[38] that this nesting is responsible for the LMAF phase. On the other hand, the incommensurate nesting, Q_h, occurs between two different orbitals, and can open a gap if a symmetry between these orbitals and spins are spontaneously broken together.[39] In what follows, the SOC eigenstate can collectively propagate with alternating sign in the total angular momentum at the wavelength determined by the modulation vector. This is the guiding instability that drives spontaneous rotational symmetry breaking, while the $\mathcal{TR}$ symmetry remains intact (see Fig. 2(a) and Ref. 39 for explanations). As the parent state is not a non-trivial topologically invariant ground-state, a gap is opened to lift the FS instability.

Low-energy effective model:- Motivated by the above-mentioned experimental results and band structure symmetry considerations, we formulate a simple and unified model by using the theory of invariants[46]. We restrict our discussions to the low-lying Γ_6 bands and neglect the unfilled Γ_8 bands. Within the j-j SOC scheme, the Γ_6 atomic states can be labeled by m_J=$\pm\frac{5}{2}$, $\pm\frac{3}{2}$, $\pm\frac{1}{2}$, where m_J is the z component of J. However, constrained by the $\mathcal{TR}$ symmetry, these states are classified into three doublets characterized by up and down 'pseudospins'. On entering into the HO state, the FS nesting commences in between the two doubly degenerate J=$\frac{3}{2}$ and J=$\frac{1}{2}$ states only.[34, 38] If no other symmetry is broken, the degenerate J=$\frac{5}{2}$ states remain unaltered in the HO state,[46] and hence they are not considered in our model Hamiltonian. Throughout this paper, we consistently use two indices: orbital index $\tau = \pm$ for $m_J = \frac{1}{2}(\frac{3}{2})$, and 'pseudospin' σ=↑(+), ↓(-) to denote their orientation. In this notation, we consider the 'pseudospinor' field $\hat{\Psi}^\dagger(\boldsymbol{k})$=($f^\dagger_{\boldsymbol{k},\frac{1}{2},+}$, $f^\dagger_{\boldsymbol{k},\frac{3}{2},+}$, $f^\dagger_{\boldsymbol{k},\frac{1}{2},-}$, $f^\dagger_{\boldsymbol{k},\frac{3}{2},-}$), where $f^\dagger_{\boldsymbol{k},\tau,\sigma}$ is the creation operator for an electron in the orbital m_J=$\frac{1}{2}$, $\frac{3}{2}$ with momentum $\boldsymbol{k}$ and 'pseudospin' σ.

The representation of the symmetry operations that belongs to the D_{4h} symmetry of the URu_2Si_2 crystal structure is: $\mathcal{TR}$ symmetry, inversion symmetry $\mathcal{I}$, four-fold rotational symmetry $\mathcal{C}_4$, and the two reflection symmetries $\mathcal{P}_{x/y}$. The SOC f-state of actinides is invariant under all symmetries except the mirror reflection, which in fact allows the formation of the SOC density wave into a finite gap in the HO state.[45] On the basis of these symmetry considerations, it is possible to deduce the general form of the non-interacting Hamiltonian

as[47]:

$$H_0 = \sum_{\boldsymbol{k},\sigma} \hat{\Psi}^\dagger(\mathbf{k}) \begin{pmatrix} h_{11}(\boldsymbol{k}) & h_{12}(\boldsymbol{k}) \\ h_{21}(\boldsymbol{k}) & h_{22}(\boldsymbol{k}) \end{pmatrix} \hat{\Psi}(\mathbf{k}), \quad (1)$$

$$h_{\tau\tau'}(\boldsymbol{k}) = \epsilon_{\tau\tau'}(\mathbf{k})\boldsymbol{\tau}^0 + \boldsymbol{d}_{\tau\tau'}(\mathbf{k}) \cdot \boldsymbol{\tau}. \quad (2)$$

Here, $\boldsymbol{\tau}^\mu$ ($\mu \in 0, x, y, z$) depict the 2D Pauli matrices in the orbital space and τ^0 is the unitary matrix ($\boldsymbol{\sigma}^\mu$) matrices will be used later to define the spin space). The $\mathcal{TR}$ invariance requires that $h_{22/21}(\boldsymbol{k})$=$h^*_{11/12}(-\boldsymbol{k})$. Under $\mathcal{TR}$ and $\mathcal{I}$ invariance, the symmetry of $\epsilon_{\tau\tau'}(\boldsymbol{k})$ and $d^{x,y,z}_{\tau\tau'}(\mathbf{k})$ must complement to their corresponding unitary and Pauli Matrix counterparts, respectively. Hence we obtain the Slater-Koster hopping terms as: $[\epsilon(\boldsymbol{k}), d^x, d^y, d^z]_{11}$ = $\big[-2t(\cos k_x + \cos k_y) - \mu,\ -2t_1 \sin k_x,\ -2t_1 \sin k_y,\ -2t_2(\cos k_x - \cos k_y)\big]$, and $[\epsilon(\mathbf{k}), d^x, d^y, d^z]_{12}$ = $\big[0, 0, 0, -4t_z \cos(k_x/2) \cos(k_y/2) \cos(k_z/2)\big]$.[48] The above Hamiltonian can be solved analytically which gives rise to four SOC energy dispersions as[47]

$$E^{\tau\sigma}(\boldsymbol{k}) = \epsilon(\boldsymbol{k}) + \tau \sqrt{\sum_\mu |\boldsymbol{d}^\mu_{12}(\mathbf{k})|^2} + \sigma \sqrt{\sum_\mu |\boldsymbol{d}^\mu_{11}(\boldsymbol{k})|^2}. \quad (3)$$

Here $\sigma = \pm$ and $\tau = \pm$ are band indices. An important difference of the present Hamiltonian with that of bulk topological insulators[3] or quantum spin-Hall systems[1] is the absence of a mass or gap parameter in the former case. The computed non-interacting bands are plotted in Fig. 2(b), which exhibit several Dirac points along the high-symmetry lines. Focusing on the Dirac point close to E_F, we find that it occurs at the crossing between bands E^{+-} and E^{-+}, demonstrating that it hosts four-fold Kramer's degeneracy (two orbitals and two spins). Therefore, lifting this degeneracy requires the presence of a SOC order parameter. However, it is important to note that the gap opening at the Dirac point is not a manifestation of the presence of degeneracy at it, but a consequence of the SOC density wave caused by FS instability.

SOC density wave induced HO:- Based on the aforementioned parent Hamiltonian, we proceed to study how the gapping takes place on the electronic structure in the HO state. The general form of a density wave order parameter including both spin and orbital quantum numbers can be written as[45]

$$M^\mu = \Big\langle \sum_{\tau\tau'\sigma\sigma'} f^\dagger_{\boldsymbol{k},\tau,\sigma} \left[\boldsymbol{b}^\mu_{\tau\tau'}(\boldsymbol{k})\boldsymbol{\sigma}^z_{\sigma\sigma'}\right] f_{\boldsymbol{k}+\boldsymbol{Q},\tau',\sigma'} \Big\rangle. \quad (4)$$

The gap vector $\boldsymbol{b}$ is defined in the orbital basis which can be expressed in term of a gap function as $\boldsymbol{b}^\mu_{\tau\tau'}(\boldsymbol{k})$=$\Delta^\mu_{\tau\tau'}(\boldsymbol{k})\boldsymbol{\tau}^\mu_{\tau\tau'}$, where the order parameter $\Delta^\mu_{\tau\tau'}(\boldsymbol{k})$ is to be calculated self-consistently with respect to its coupling constant (see Ref. 45). Eq. 4 admits a plethora of order parameters related to the SOC density wave formations which break symmetry in different ways. Among them, we rule out those parameters which render gapless states by using the symmetry arguments[45, 49]: All four order parameters obey inversion symmetry, while only M^y term is even under time-reversal, because it is the product of two odd terms $\boldsymbol{\tau}^y$ and $\boldsymbol{\sigma}$ (we drop the superscript 'y' henceforth). This is the only term which commences a finite gap opening if the translational or rotational symmetry is spontaneously broken. We have shown in Ref. 45 that there is a considerably large parameter space of the coupling constant where this order parameter dominates.

Eq. 4 implies that spin and orbital orderings occur simultaneously along the 'hot-spot' direction $\boldsymbol{Q}$,[51] as illustrated in Fig. 2(a). It propagates along $\boldsymbol{Q}_x$ or $\boldsymbol{Q}_y$ directions with alternating signs (particle-hole pairs) to commence a SOC density wave. The resulting Hamiltonian breaks the four-fold rotational symmetry down to a two-fold one $\mathcal{C}_2$, and gives rise to a so-called spin-orbit 'nematic' state.[50] The present SOC order parameter is microscopically distinct with the existing order parameters, see Ref. 51. Taking into account the band-structure information that $\boldsymbol{Q}_h$ represents the interband nesting, it is instructive to focus on only $\boldsymbol{b}_{12}(\boldsymbol{k})$ component (thus the subscript '12' is eliminated hereafter). Therefore, the SOC density wave does not introduce a spin or orbital moment, but a polarization in the total angular momentum Δm_J=± 2 [for the ordering between $\frac{3}{2}$(-$\frac{3}{2}$) and -$\frac{1}{2}$($\frac{1}{2}$), respectively]. This value agrees remarkably well with Neutron experiment data of $g\mu_B\langle J_z\rangle \approx 2\mu_B$ (bare Landgé g factor is $\sim$0.8 for $5f$ states of U-atom[52]) at the same incommensurate vector $\boldsymbol{Q}_h$. [18] We discuss below and in Ref. 45 the experimental implications of this polarization vector.

The $\boldsymbol{b}$ vector belongs to the same irreducible point group representation, E_g, of the crystal with odd parity, and can be defined by $|\boldsymbol{b}(\boldsymbol{k})|$=$2i\Delta^x \sin k_x a$, or $2i\Delta^y \sin k_y a$ for the nestings along $\boldsymbol{Q}^x_h = (1.4, 0, 0)$, or $\boldsymbol{Q}^y_h = (0, 1.4, 0)$, respectively. The mean-field Hamiltonian for the HO state within an effective two band model reduces to the general form H_{MF}=H_0+H_{SOC}, where the particle-hole coupling term is

$$H_{SOC} = 2i \sum_{\boldsymbol{k}} \sum_{\mu=x,y} \Delta^\mu \sin(k_\mu a) f^\dagger_{\boldsymbol{k},1,\uparrow} f_{\boldsymbol{k}+\boldsymbol{Q}^i_h,2,\downarrow} + h.c. \quad (5)$$

The 'hot-spot' vector divides the unit cell into a reduced 'SOC Brillouin zone' in which we can define the Nambu operator in the usual way $\Big(\hat{\Psi}^\dagger(\boldsymbol{k}),\ \hat{\Psi}^\dagger(\boldsymbol{k}+\boldsymbol{Q}^x_h),\ \hat{\Psi}^\dagger(\boldsymbol{k}+\boldsymbol{Q}^y_h)\Big)$. In this Nambu representation, it is obvious that the HO term merely adds a mass term into the d^y_{12} term defined above. At the Dirac points located where $|\boldsymbol{d}^2_{12}|$-$|\boldsymbol{d}^2_{11}|$=0, a gap opens by $|\boldsymbol{b}(\boldsymbol{k})|^2$.

*SOC gap opening and topological properties:-*Figure 2 demonstrates the development of the quasi-particle structure in the HO state. The topological property of the HO state is evaluated by using Fu and Kane classification scheme,[2] as done extensively in the literature.[3, 5–7] They have shown that if the Z_2 number (product of the parity of all filled states) of a system under $\mathcal{TR}$ and $\mathcal{I}$ is -1, the system is topologically non-trivial. URu_2Si_2 is topologically trivial above the HO state, i.e., $Z^0_2 = +1$. The gap opening makes the top of the valence band (odd parity) to drop below E_F as shown in Fig. 2(b). Thereby, an odd parity gained in the occupied level endows the system to a non-trivial topological order phase: $Z_2 = Z^0_2 \times (-1) = -1$. This behavior is fully consistent with the band progression and the associated gap open-

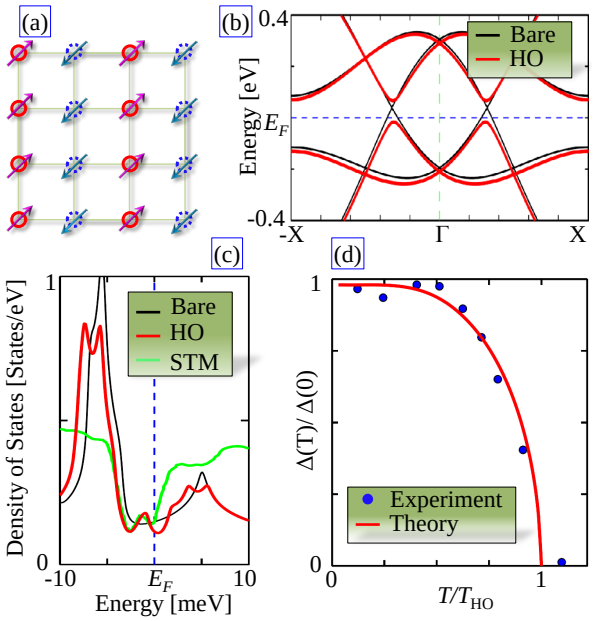

FIG. 2. (a) A typical form of the SOC nematic order is schematically described for an illustrative case of commensurate nesting. The solid and dashed circles encode two opposite orbitals, $\tau = \pm$, where the associated arrows depict their 'pseudospins' σ. Both $\boldsymbol{\tau}$ and $\boldsymbol{\sigma}$, representing orbital and spin respectively, individually break $\mathcal{TR}$ symmetry, while their product remains $\mathcal{TR}$ invariant.[39] (b) Model dispersions of the $|\pm\frac{1}{2}\rangle$, and $|\pm\frac{3}{2}\rangle$ subbands plotted along the axial direction. Black and red lines give dispersion before and after including the HO gap, respectively. An artificially large value of Δ=50 meV is chosen here to clearly explicate the momentum dependence of the modulated SOC gap opening. (c) Modifications of DOS upon entering into the HO phase are compared with measured DOS in the STM experiment (green line).[14] Note that the experimental data is subtracted from the background spectrum at $T>T_h$, which helps highlight the appearance of multiple structures in the DOS spectrum at the HO state. Here the gap magnitude $\Delta(0)$ is 5 meV, obtained at a coupling strength of 27 meV, see Ref. [45]. (d) The self-consistent value of $\Delta(T)$ exhibits the mean-field behavior of the HO gap, in consistent with experiments.[9] We obtain $T_{HO} = 22$ K which is larger than the experimental value of $T_{HO} = 17.5$ K. However, recently it has been pointed out that there exists a 'pseudogap' above the HO state,[53] which presumably reduces the mean-field temperature scale.

ing observed by angle-resolved photoemission spectroscopy (ARPES)[15, 16] upon entering into the HO phase. The scanning tunneling microscopy and spectroscopic (STM/S)[9, 14] fingerprints of the gap opening in the density of state (DOS) is also described nicely within our calculations, see Fig. 2(c).

QCP:-One way to characterize the nature of a phase transition is to determine the temperature evolution of the gap value. Our computed self-consistent values of the mean-field gap $\Delta(T)$ agree well with the extracted gap values from the STM spectra[9] (after rescaling the T_{HO} value[45]). This mean-field behavior is also qualitatively consistent with the mean-field like jump observed in numerous bulk properties, including specific heat,[10] resistivity,[11] linear[10] and nonlinear[12] susceptibilities, thermal expansion[13]. A calculation of these bulk properties is, however, necessary to quantify how much jump is accounted for by this order parameter.[47] Furthermore, the HO gap is topologically protected from any $\mathcal{TR}$ invariant perturbation such as pressure (with sufficient pressure the HO transforms into the LMAF phase), while $\mathcal{TR}$ breaking perturbation such as magnetic field will destroy the order. Remarkably, these are the hallmark features of the HO states,[23, 34, 54] which find a natural explanation within our topological density wave order scenario. In what follows, the magnetic field will destroy the HO state even at $T = 0$ K, that means at a quantum critical point (QCP).[55] Identifying location of the QCP is beyond the scope of the present work. However, with the help of the experimental data from Ref. 54, we find that a QCP resides around $B = 33$ T (see Ref. [45]). On the basis of these results, we attribute the HO phase transition to be associated with a 'topological quantum critical point' which encodes a second order quantum phase transition as a function the magnetic field, as well as a trivial to non-trivial topological phase transition at the same time.

Testable predictions:-As definite tests of the $\mathcal{TR}$ invariant SOC order parameter, we propose two measurements. (1) We predict an inelastic neutron scattering (INS) mode with enhanced intensity at $\boldsymbol{Q}_h$ near $\omega \sim 8 - 10$ meV below T_{HO}, see Ref. 45 for calculation. Although, INS measurement has observed a gap opening at this momentum,[37] however, a polarized INS measurement in the longitudinal channel will be of considerable value to distinguish our proposed $\mathcal{TR}$ invariant mode from any spin-flip and elastic background.[56] (2) The consequence of a topological bulk gap is the presence of surface states.[2] In our present model, we expect two surface states of opposite spin connecting different orbitals inside the HO gap.[47] Of course, due to the even number of surface Dirac states, it is unlikely to be topologically protected. The chirality of the surface state can be probed by ARPES using circular polarized light.

Conclusions: Our calculations, in quantitative agreement with numerous experimental observations, provide a microscopic explanation for the origin of the HO state in URu_2Si_2. The spin-orbit locked f-states develop a paramount FS nesting instability, whose feedback effect renders into a modulated SOC density wave that propagates along the unidirectional 'hot-spot' direction. A mean-field like 'nematic order' thereby emerges in the HO phase, which is, in fact, a hallmark feature of any four-fold symmetry breaking systems.[23, 34] The order parameter produces a polarized total angular momentum Δm_J=$\pm$2, which is in excellent agreement with INS data.[18] We propose a $\mathcal{TR}$ invariant INS mode, and chiral surface states as two testable properties for this SOC induced HO state. The results suggest that the quantum and topological phase transition together defines a topological second-order phase transition accompanied by a 'topological quantum critical point'. The present SOC density wave is a new state of matter which can also be looked for in other classes of material possessing strong SOC and time-reversal symmetry.

I thank A. V. Balatsky, M. J. Graf, A. Bansil, R. S. Markiewicz, T. Durakiewicz, C. Batista for stimulating discussions. I am indebted to J.-X. Zhu for sharing the input file for URu_2Si_2 for first-principles calculations. I am grateful to P. M. Oppeneer for pointing out the experimental value of Δm_J which agrees well with our present theory. I thank J. Haraldsen and T. Ahmed for critical reading of this paper. This work was funded by US DOE, BES and LDRD and benefited from the allocation of supercomputer time at NERSC.

[1] B. A. Bernevig, *et al.*, Science **314**, 1757 (2006).
[2] L. Fu, *et al.*, Phys. Rev. Lett. **98**, 106803 (2007).
[3] H. Zhang *et al.*, Nature Physics **5**, 438 (2009).
[4] D. Hsieh *et al.*, Nature **460**, 1101 (2009).
[5] S. Raghu *et al.*, Phys. Rev. Lett. **100**, 156401 (2008).
[6] M. Dzero *et al.*, Phys. Rev. Lett. **104**, 106408 (2010).
[7] R. S. K. Mong, *et al.*, Phys. Rev. B **81**, 245209 (2010).
[8] J. A. Mydosh, and P. M. Oppeneer, Rev. Mod. Phys., **83** 1301-1322 (2011).
[9] P. Aynajiana *et al.*, Proc. Nat. Aca. Sci. USA **107**, 10383 (2010).
[10] T. T. M. Palstra *et al.*, Phys. Rev. Lett. **55**, 2727 (1985).
[11] T. T. M. Palstra, *et al.*, Phys. Rev. B **33**, 6527 (1986).
[12] A. P. Ramirez *et al.*, Phys. Rev. Lett. **68**, 2680 (1992).
[13] A. De Visser *et al.*, Phys. Rev. B **34**, 8168 (1986).
[14] A. R. Schmidt *et al.*, Nature **465** (2010).
[15] A. F. Santander-Syro *et al.*, Nat. Phys. **5**, 637 (2009).
[16] R. Yoshida *et al.*, Phys. Rev. B **82**, 205108 (2010).
[17] T. E. Mason, and W. J. L. Buyers, Phys. Rev. B **43**, 11471 (1991).
[18] C. Broholm *et al.*, Phys. Rev. B **43**, 12809 (1991).
[19] S. A. M. Mentink *et al.*, Phys. Rev. B **5**3, 6014(R) (1996).
[20] P. Chandra, *et al.* Nature **417**, 831-834 (2002).
[21] H. Amitsuka *et al.*, Phys. Rev. Lett. **83**, 5114 (1999).
[22] R. A. Fisher *et al.*, Physica B **163**, 419 (1990).
[23] R. Okazaki *et al.*, Science **331**, 439 (2011).
[24] Existing theories include multiple spin correlator[57], Jahn-Teller distortions[25], unconventional spin-density wave,[26, 27], antiferromagnetic fluctuation,[28] orbital order, [20], helicity order,[29], staggered quadrupole moment[30], octupolar moment,[31] hexadecapolar order,[32], linear antiferromagnetic order,[38] incommensurate hybridization wave,[33] among others[8].
[25] T. Kasuya, *et al.*, J. Phys. Soc. Jpn. **66**, 3348 (1997).
[26] H. Ikeda, and Y. Ohashi, Phys. Rev. Lett. **81**, 3723 (1998).
[27] V. P. Mineev, and M. E. Zhitomirsky, Phys. Rev. B **72**, 014432 (2005).
[28] Y. Okuno, and K. Miyake, J. Phys. Soc. Jpn. **67**, 2469 (1998).
[29] C. M. Varma, and L. Zhu, Phys. Rev. Lett. **96**, 036405 (2006).
[30] P. Santini, Phys. Rev. B **57**, 5191-5199 (1998).
[31] K. Hanzawa, J. Phys.: Condens. Matter **19**, 072202 (2007).
[32] K. Haule, and G. Kotliar, Nat. Phys. **5**, 796-799 (2009); H. Kusunose, and H. Harima, J. Phys. Soc. Jpn. **80**, 084702 (2011).
[33] Y. Dubi, and A. V. Balatsky, Phys. Rev. Lett. **106**, 086401 (2011).
[34] S. Fujimoto, Phys. Rev. Lett. **106**, 196407 (2011).
[35] C. Pépin *et al.*, Phys. Rev. Lett. **106**, 106601 (2011).
[36] P. M. Oppeneer *et al.*, Phys. Rev. B **84**, 241102(R) (2011).
[37] C. R. Wiebe *et al.*, Nat. Phys. **3**, 96 (2007).
[38] S. Elgazzar, *et al.*, Nat. Mat. **8**, 337-341 (2009).
[39] In URu_2Si_2, $SU(2)$ symmetry can not be defined for spin or orbital alone, as they are coupled to each other via SOC. Therefore, the 'parent' Hamiltonian has to be defined in $SU(2) \otimes SU(2)$ representation. Both $SU(2)$ groups, separately are odd under $\mathcal{TR}$, but their product $SU(2) \otimes SU(2)$ becomes even.
[40] P. Blaha *et al.*, An augmented plane wave plus local orbitals program for calculating crystal properties. *(Techn. Univ. Wien,* (2001).
[41] J. P. Perdew, *et al.*, Phys. Rev. Lett. **77**, 3865 (1996).
[42] J. D. Denlinger *et al.*, J. Elect. Spect. Relat. Phenom. **117**, 347 (2001).
[43] T. Hotta, and K. Ueda, Phys. Rev. B **67**, 104518 (2003).
[44] These nesting vectors transform properly to the body-center tetragonal crystal defined in which Q_2 obtain the well-know value of $(0, 0, 1)$.
[45] See attached Supplementary Materials for details.
[46] R. Winkler, Spin-orbit coupling effects in two dimensional electron and hole systems. *(Springer Tracts in Modern Physics, Vol. 191, Springer* (2003).
[47] Tanmoy Das, under preparation.
[48] The obtained values of the tight-binding hopping parameters as $t = -45$, $t_1 = -45$ meV, $t_2 = -50$ meV, $t_z = 25$ meV.
[49] Y. Ran *et al.*, Phys. Rev. B **79**, 014505 (2009).
[50] J. Zaanen, and O. Gunnarsson, Phys. Rev. B **40**, 7391-394 (1989); S. A. Kivelson, E. Fradkin, and V. J. Emery, Nature **393**, 550-553 (1998).
[51] The present $\mathcal{TR}$ invariant SOC order parameter is inherently distinct from any $\mathcal{TR}$ breaking spin or orbital order.[39] This criterion also rules out any similarly between our present spin-orbit nematic state with the spin-nematic phase[34] or spin-liquid state[35]. Furthermore, the present order parameter is different from $\mathcal{TR}$ invariant 'hybridization wave' (between f and d orbitals of same spin), or charge density wave or others,[30, 32] as SOC order involves flipping of both orbital (between split f orbitals that belong to Γ_6 symmetry) and spin simultaneously.
[52] Of course, interaction can increase the value of the 'g-factor', which may give even a better agreement of the computed value of Δm_J with the measured one.
[53] J. T. Haraldsen, *et al.* Phys. Rev. B **84**, 214410 (2011).
[54] K. H. Kim *et al.*, Phys. Rev. Lett. **91**, 256401 (2003); J. Levallois *et al.*, Europhys Lett. **85**, 27003 (2009).
[55] S. Sachdev, Quantum phase transitions, *Cambridge University Press, Cambridge U.K.* (1999).
[56] B. Fauqué, *et al.* Phys. Rev. Lett. **96**, 197001 (2006).
[57] V. Barzykin, and L. P. Gor'kov, Phys. Rev. Lett. **70**, 2479 (1993).

Supplementary Material for "Hidden topological order in the heavy fermion metal URu_2Si_2"

Tanmoy Das[1,2]
[1]*Theoretical Division, Los Alamos National Laboratory, Los Alamos, NM, 87545, USA.*
[2]*Physics Department, Northeastern University, Boston, MA, 02115, USA.*
(Dated: February 6, 2012)

PACS numbers: 71.27.+a,03.65.Vf,74.40.Kb,75.25.Dk

In the main text, we have provided an effective two band model which is relevant for the study of hidden-order (HO) gap structure coming from Fermi surface (FS) nesting. Here, we expand on how such an effective Hamiltonian is deduced. The spin-orbit splitting state is studied, in general, within either $\boldsymbol{L}.\boldsymbol{S}$ coupling or $j-j$ coupling approaches. In the former case, the total $\boldsymbol{L}$ and $\boldsymbol{S}$ quantum states are formed due to strong Hund's coupling prior to the formation of spin-orbit coupled eigenstates. Such process occurs in insulating compounds with localized f states.[1] However, in actinides the spin-orbit interaction is stronger than the Hund's coupling. Therefore, total angular momentum $\boldsymbol{J}=\boldsymbol{L}+\boldsymbol{S}$ becomes the good quantum number for this state. However, due to finite Hund's coupling, the term $\boldsymbol{L}.\boldsymbol{S}$ becomes active at some critical value of the coupling constant by taking advantage of any instability, such as FS nesting [shown in supplementary Fig. 1(a)], even when the time-reversal symmetry remains invariant. Therefore, we desire to study a Hamiotnian:

$$H = H_0 + H_{SOC}, \tag{1}$$

where H_0 is the non-interacting part and H_{SOC} is the spin-orbit coupling (SOC) term. In the 'pseudospin' basis $\hat{\Psi}^\dagger(\boldsymbol{k}) = (f^\dagger_{\boldsymbol{k},\frac{1}{2},\sigma},\ f^\dagger_{\boldsymbol{k},\frac{3}{2},\sigma}, f^\dagger_{\boldsymbol{k},\frac{1}{2},\bar{\sigma}},\ f^\dagger_{\boldsymbol{k},\frac{3}{2},\bar{\sigma}})$ ($\bar{\sigma}=-\sigma$), the representation of the symmetry operations for URu_2Si_2 which belongs to the D_{4h} symmetry is: time-reversal symmetry $\mathcal{TR} = \mathcal{K}\cdot i\boldsymbol{\sigma}^y\otimes\boldsymbol{\tau}^0$, inversion symmetry $\mathcal{I}=\boldsymbol{\tau}^z\otimes\boldsymbol{\tau}^0$, four-fold rotational symmetry around the z axis $\mathcal{C}_4 = \exp\left[i(\pi/4)\boldsymbol{\sigma}^z\otimes\boldsymbol{\tau}^0\right]$ and the two reflection symmetries $\mathcal{P}_{x/y} = i\boldsymbol{\sigma}^{x/y}$ which map $x\rightarrow -x$ (where x is in Γ-X direction) and $y\rightarrow -y$ (where y is orthogonal to Γ-X direction), respectively. Here, $\mathcal{K}$ is complex conjugation operator, and $\boldsymbol{\sigma}^{x,y,z}$ and $\boldsymbol{\tau}^{x,y,z}$ depict the 2D Pauli matrices in the 'pseudospin' and orbital space, respectively where $\boldsymbol{\tau}^0=\boldsymbol{\sigma}^0$ are the unitary matrices.

Each symmetry operation transforms the time-reversal invariant f-electron field as:

$$\mathcal{I}\hat{\Psi}(k_x,k_y) \rightarrow -\boldsymbol{\tau}^0\hat{\Psi}(-k_x,-k_y), \tag{2}$$

$$\mathcal{C}_4\hat{\Psi}(k_x,k_y) \rightarrow i\boldsymbol{\tau}^y\hat{\Psi}(-k_y,k_x), \tag{3}$$

$$\mathcal{P}_{x/y}\hat{\Psi}(k_x,k_y) \rightarrow \mp\boldsymbol{\tau}^z\hat{\Psi}(\mp k_x,\pm k_y). \tag{4}$$

These symmetry operations imply that the SOC actinide f-state is an odd-parity wavefunction. Using these symmetry properties, the non-interacting Hamiltonian is derived in the main text, using standard procedure, see for example Refs. 2 and 3.

HIDDEN ORDER PARAMETER

Considering the non-interacting FS nesting at $\boldsymbol{Q}_h = (1\pm 0.4, 0, 0)$ for the HO state as demonstrated in the main text, we expand the above-mentioned 'pseudospinor' in the Nambu notation as $\hat{\Psi}(\boldsymbol{k}) = \left(\hat{\Psi}(\boldsymbol{k}), \hat{\Psi}(\boldsymbol{k}+\boldsymbol{Q})\right)$. In this notation, the mean-field interaction term can be written in general as

$$H_{SOC} = \sum_{\mu\mu'} g^{\mu\mu'}\Gamma^{\mu\mu'}\hat{\Psi}^\dagger(\boldsymbol{k})\Gamma^{\mu\mu'}\hat{\Psi}(\boldsymbol{k}+\boldsymbol{Q}), \tag{5}$$

where $\mu,\mu'\in\{0,x,y,z\}$. Here g is the coupling constant discussed latter and $\Gamma_{\mu\mu' u} = \boldsymbol{\tau}^\mu\otimes\boldsymbol{\sigma}^{\mu'}$. Absorbing g and Γ into one term, we define the mean-field order parameter

$$M_{\mu\nu} = g_{\mu\nu}(\boldsymbol{k})\left\langle\hat{\Psi}(\boldsymbol{k})^\dagger\boldsymbol{\tau}^\mu\otimes\boldsymbol{\sigma}^\nu\hat{\Psi}(\boldsymbol{k}+\boldsymbol{Q})\right\rangle. \tag{6}$$

$$= g_{\mu\nu}(\boldsymbol{k})\left\langle f^\dagger_{\boldsymbol{k},\tau,\sigma}\boldsymbol{\tau}^\mu_{\tau\tau'}\otimes\boldsymbol{\sigma}^\nu_{\sigma\sigma'}f_{\boldsymbol{k}+\boldsymbol{Q},\tau',\sigma'}\right\rangle. \tag{7}$$

Here τ,τ' and σ,σ' (not in bold font) are the components of the $\boldsymbol{\tau}^\mu$ and $\boldsymbol{\sigma}^\nu$ matrices, respectively. Without any loss of generality we fix the spin orientation along z-directions ($\mu'=z$). Therefore, we drop the index μ' henceforth. Furthermore we define the gap vector as

$$\boldsymbol{b}^\mu_{\tau\tau'}(\boldsymbol{k}) = \Delta^\mu_{\tau\tau'}(\boldsymbol{k})\boldsymbol{\tau}^\mu_{\tau\tau'},\quad \Delta^\mu_{\tau\tau'}(\boldsymbol{k}) = g_{0\tau\tau'}\boldsymbol{\phi}(\boldsymbol{k}), \tag{8}$$

where $\boldsymbol{\phi}(\boldsymbol{k})$ is the structure factor for the gap function which transforms according to the same irreducible representation of the point-group symmetry. The D_{4h} symmetry of the crystal implies that the gap function belongs to 1D E_g symmetry: $\boldsymbol{\phi}(\boldsymbol{k}) = (\sin k_x, \sin k_y)$. Substitution these terms in Eq. 7, we obtain the final expression for the order parameter as

$$M^\mu = \left\langle\sum_{\tau\tau'\sigma\sigma'} f^\dagger_{\boldsymbol{k},\tau,\sigma}\left[\boldsymbol{b}^\mu_{\tau\tau'}(\boldsymbol{k})\boldsymbol{\sigma}^z_{\sigma\bar{\sigma}}\right]f_{\boldsymbol{k}+\boldsymbol{Q},\tau',\bar{\sigma}}\right\rangle. \tag{9}$$

This is the term given in the main text in Eq. 4.

All the symmetry properties of the order parameters are given in Table I. For the unidirectional modulation vector $\boldsymbol{Q}_h$, all components of M^μ break C_4 rotational symmetry. M^0, M^x and M^z break time-reversal and thus are ruled out as the hidden-order state is arguably does not exhibit any time-reversal symmetry breaking.[4–6]. Although some experimental evidences for the time-reversal symmetry breaking are also present, but it is not well established if the measurements are done in single crystal where the time-reversal symmetry breaking LMAF state and time-reversal symmetry invariant

	M^0	M^x	M^y	M^z
$\mathcal{TR}$	-	-	+	-
$\mathcal{C}_4$	-	-	-	-
$\mathcal{I}$	+	+	+	+
$\mathcal{P}_{x/y}$	+	-	-	+

TABLE I. Symmetry properties of various density wave parameters. '+' ('-') represent 'even' ('odd') parity of the order parameter under the corresponding symmetry operation.

HO state are not mixed. In the microscopic sense, LMAF and HO state are separated by phase transition, and thus both phases cannot inherit same broken symmetry.

On the other hand, M^y is even under time-reversal but odd under parity, and thus adds a mass term to the Hamiltonian which opens a gap at the nested portion of the FS. This is the term that represents modulated SOC. A trivial check can be performed by explicitly writing down the the spin-orbit coupling term $\sum_i (-1)^{i_x} L_{i,z} S_{i,z} \propto f^\dagger_{i,+,\sigma} f_{i,+,\sigma'} - f^\dagger_{i,-,\sigma} f_{i,-,\bar{\sigma}} = 2i f^\dagger_{i,\frac{1}{2},\sigma} f_{i,\frac{3}{2},\bar{\sigma}} + h.c.$, where we have substituted $f_{i,\pm,\sigma} = (f_{i,\frac{1}{2},\sigma} \pm i f_{i,\frac{3}{2},\sigma})$ and $\bar{\sigma} = -\sigma$.

SOC CORRELATION FUNCTIONS

The non-interacting single-particle Green's function for the Hamiltonian given in Eq. 1 above is defined as $G^{-1}(\boldsymbol{k}, i\omega_n) = -1/\beta \sum_n \langle T_\mathcal{T} f_{\boldsymbol{k}\tau\sigma}(\mathcal{T}) f^\dagger_{\boldsymbol{k}\tau'\sigma'}(0) \rangle e^{i\omega_n \mathcal{T}} = i\omega_n - H(\boldsymbol{k})$. Here $\mathcal{T}$ is the imaginary time, $f_{\boldsymbol{k}\tau\sigma}(\mathcal{T})$ is the imaginary time evolution of the fermionic operator $f_{\boldsymbol{k}\tau\sigma}$, n is the fermionic Matsubara frequency, and $\beta = 1/k_B T$ (k_B is Boltzmann constant). $T_\mathcal{T}$ gives normal time ordering. The anomalous part of the Green's function is

$$F^\mu_{\tau\tau'\sigma\sigma'}(\boldsymbol{k}, i\omega_n) = -\frac{1}{\beta} \sum_n \left\langle T_\mathcal{T} f_{\boldsymbol{k},\tau\sigma}(\mathcal{T}) f^\dagger_{(\boldsymbol{k}+\boldsymbol{Q}),\tau'\sigma'}(0) \right\rangle e^{i\omega_n \mathcal{T}},$$
$$= \sum_\nu R^\nu_{\tau\tau'\sigma\sigma'}(\boldsymbol{k}) \frac{|\Delta^\mu_{\tau\tau'}|}{(i\omega_n)^2 - (E^{\tau\sigma}_{\boldsymbol{k},\nu})^2}, \quad (10)$$

The quasiparticle states are: $E^{\tau\sigma}_{\boldsymbol{k},\nu} = \xi^{\tau\sigma}_{\boldsymbol{k}+} + \nu E^{\tau\sigma}_{\boldsymbol{k},0}$, and $E^{\tau\sigma}_{\boldsymbol{k},0} = \sqrt{(\xi^{\tau\sigma}_{\boldsymbol{k}-})^2 + |\Delta^\mu_{\tau\tau'}|^2}$, where $\xi^{\tau\sigma}_{\boldsymbol{k}\pm} = (E^{\tau\sigma}_{\boldsymbol{k}} \pm E^{\tau\sigma}_{\boldsymbol{k}+\boldsymbol{Q}})/2$, and $E^{\tau\sigma}_{\boldsymbol{k}}$ is defined in the main text in Eq. 3. $\nu, \nu' = \pm$. The corresponding coherence factors are $u_{\boldsymbol{k}}(v_{\boldsymbol{k}}) = 1/2(1 \pm \xi^{\tau\sigma}_{\boldsymbol{k}-}/E^{\tau\sigma}_{\boldsymbol{k},0})$. The orbital overlap matrix-element $R^\nu_{\tau\tau'\sigma\sigma'}(\boldsymbol{k}) = \psi^\nu_{\tau\sigma}(\boldsymbol{k}) \psi^{\nu\dagger}_{\tau'\sigma'}(\boldsymbol{k})$, where ψ is the eigenvector of the noninteracting Hamiltonian.

The general form of the polarization vector for the SOC density wave is $J^z_{\tau\tau'\sigma\sigma'}(\boldsymbol{q}, \mathcal{T}) = \sum_{\boldsymbol{k}} f^\dagger_{\boldsymbol{k},\tau,\sigma}(\mathcal{T}) \boldsymbol{\tau}^\mu_{\tau\tau'} \boldsymbol{\sigma}^z_{\sigma\sigma'} f_{\boldsymbol{k}+\boldsymbol{q},\tau',\sigma'}(\mathcal{T})$. To simplify the notations, let us define composite indices $\alpha, \beta = \tau\tau'\sigma\sigma'$, in which the correlation function of J^z_α vector can now be defined as

$$\chi^{zz}_{\alpha\beta}(\boldsymbol{q}, \mathcal{T}) = \frac{1}{N} \left\langle T_\mathcal{T} J^z_\alpha(\boldsymbol{q}, \mathcal{T}) J^z_\beta(-\boldsymbol{q}, 0) \right\rangle. \quad (11)$$

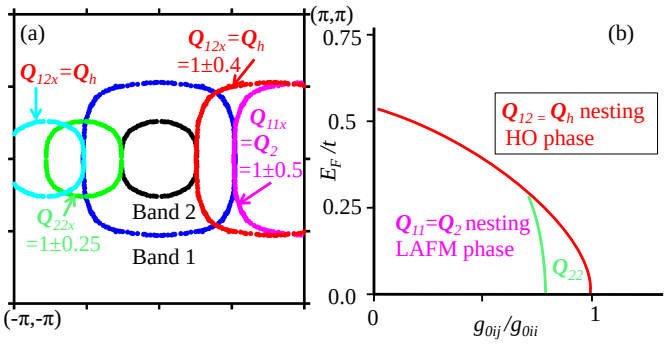

FIG. 1. (a) Black symbols are *ab-initio* FS, as shown in Fig. 1 of main text, but only two relevant bands are plotted here. The large FS for band 1 is shifted along the $x-$direction by nesting vectors $\boldsymbol{Q}_{11} = \boldsymbol{Q}_2$ and $\boldsymbol{Q}_{12} = \boldsymbol{Q}_h$. The small FS for band 2 is shifted along $-x$ direction by $\boldsymbol{Q}_{22}$ and $\boldsymbol{Q}_{12}$. Good nestings for all three vectors are observed. The intraband nestings, $\boldsymbol{Q}_{11/22}$ are, however, protected by strong SOC, where the HO nesting $\boldsymbol{Q}_{12}$ is allowed to open a gap under $\mathcal{TR}$. (b) Phase diagram as a function of intra-orbital ($g_{0ij} = g_{012} = g_{021}$) and inter-orbital coupling constant ($g_{0ii} = g_{011}, g_{022}$) and nearest neighbor hopping (t) with respect to the Fermi energy (E_F) for all thee nesting instabilities. We find that for smaller inter-orbital coupling than the intra-orbital one, the hidden order parameter arises if E_F/t ration is large. With large t (proportional to pressure), the LMAF phase at the commensurate nesting wins. This result is consistent, at least in qualitative level, with the phase diagram of URu_2Si_2[7], see Fig. 3.

Substituting J^z_α and then applying standard Wick's decomposition to the electron bracket[8] yields,

$$\chi^{zz}_{\alpha\beta}(\boldsymbol{q}, ip_m) = -\frac{1}{N} \sum_{\boldsymbol{k},n} [G_\alpha(\boldsymbol{k}, i\omega_n) G_\beta(\boldsymbol{k}+\boldsymbol{q}, i\omega_n + ip_m)$$
$$- F_\alpha(\boldsymbol{k}, i\omega_n) F_\beta(\boldsymbol{k}+\boldsymbol{q}, i\omega_n + ip_m)]. \quad (12)$$
$$= \frac{1}{N} \sum_{\boldsymbol{k}} S_{\alpha\beta}(\boldsymbol{k}, \boldsymbol{q}) \quad (13)$$
$$\times \Big[(u_{\boldsymbol{k}} u_{\boldsymbol{k}+\boldsymbol{q}} + v_{\boldsymbol{k}} v_{\boldsymbol{k}+\boldsymbol{q}})^2 (\chi^{++} + \chi^{--})$$
$$+ (u_{\boldsymbol{k}} v_{\boldsymbol{k}+\boldsymbol{q}} - v_{\boldsymbol{k}} u_{\boldsymbol{k}_{\boldsymbol{q}}})^2 (\chi^{+-} + \chi^{-+}) \Big] \quad (14)$$

Here $S_{\alpha\beta}(\boldsymbol{k}, \boldsymbol{q}) = R_\alpha(\boldsymbol{k}) R_\beta(\boldsymbol{k}+\boldsymbol{q})$ is the matrix-element term which projects the susceptibility from the band representation to the orbital one. $\chi^{\nu\nu'}$ are the fermionic oscillator terms in the band space $\nu, \nu' = \pm$:

$$\chi^{\nu\nu'}(\boldsymbol{k}, \boldsymbol{q}, i\omega_n) = -\frac{n^\nu_f(\boldsymbol{k}) - n^{\nu'}_f(\boldsymbol{k}+\boldsymbol{q})}{i\omega_n - E^\nu_{\boldsymbol{k}} - E^{\nu'}_{\boldsymbol{k}+\boldsymbol{q}}}. \quad (15)$$

$n^\nu_f(\boldsymbol{k})$ is the fermion distribution function.

HIDDEN ORDER INSTABILITY

The divergence in the real-part of the $\chi_{\alpha\beta}(\boldsymbol{q}, \omega = 0)$ indicates an instability due to the FS nestings between two orbitals α and β (in the explicit notation χ_{11} means χ_{1111}, etc).

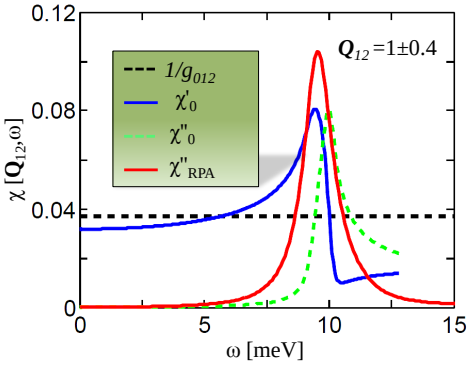

FIG. 2. The real and imaginary part of the bare susceptibility calculated from Eqs. 14-15 in the HO state. The red line gives the INS mode obtained using RPA calculation at $g_{012} = 27$ meV at which the gap is evaluated self-consistently to be $\Delta = 5$ meV. The RPA value has a huge peak (resonance), and we have rescaled its intensity arbitrarily to fit it into the same figure with bare susceptibilites.

The two intraband nestings at Q_{11} and Q_{22} can give rise to spin-density wave or antiferromagnetism, if the time-reversal symmetry is broken. We believe that Q_{11} is responsible for the LMAF phase. Our present interest is the interband one at Q_{12}, shown in supplementary Fig. 1(a) which happens at $(1 \pm 0.4, 0, 0)$. Since in this case, both orbital and spin flip together, the time-reversal symmetry remains intact.

The corresponding critical value of the coupling constants $g_{0\alpha\beta}$ at which an order parameter develops can be evaluated within random-phase approximation (RPA). The stoner criterion for an instable state implies that $1-\chi'_{\alpha\beta}(\boldsymbol{Q}_{\alpha\beta},0)g_{0\alpha\beta} \geq 0$, or $g_{0\alpha\beta} \leq 1/\chi'_{\alpha\beta}(\boldsymbol{Q}_{\alpha\beta},0)$. Looking at the FS areas for each band, shown in supplementary Fig. 1(a), we immediately see that $1/\chi'_{11}(\boldsymbol{Q}_{11},0) < 1/\chi'_{22}(\boldsymbol{Q}_{22},0) < 1/\chi'_{12}(\boldsymbol{Q}_{12},0)$, leading to a phase diagram shown in supplementary Fig. 1(b). The present calculation does not incorporate the possible coexistence state between different phases. The phase diagram implies that there is a considerably large parameter space, where the $\boldsymbol{Q}_{12} = \boldsymbol{Q}_h$ nesting dominates. We have not considered the possible phases within Q_{12} nesting discussed in Eq. 9 above, because constrained by the symmetry arguments given in Table I, all orders except M^y render gapless state.

NEUTRON MODE AT THE HIDDEN ORDER STATE

Eqs. 14 and 15, imply that the HO transition accompanies an inelastic neutron scattering mode with enhanced intensity at Q_{12} whose energy scale is approximately given by $\chi''(\boldsymbol{Q}_{12},\omega) \sim C\delta(\omega - E^1_{\boldsymbol{k}} - E^2_{\boldsymbol{k}+\boldsymbol{Q}}) \approx C\delta(\omega - |\Delta(\boldsymbol{k})| - |\Delta(\boldsymbol{k}+\boldsymbol{Q})|)$. C is the prefactor which has to be evaluated rigorously, but it does not contribute to the peak position in bare χ''. Here we have substituted the condition that non-interacting bands are nested on the FS at Q_{12} such as $E^\nu_{\boldsymbol{k}} = |\Delta(\boldsymbol{k})| \approx$5 meV. The RPA correction shifts the energy scale slightly below its bare value, and a resonance arises at $\omega_{res} \sim$9 meV, see Fig. 2. INS measurement has observed a gap opening at this nesting vector.[9] However, one have to be careful to directly compare our result with this data. Because, in the present case, we expect a mode which does not break time-reversal symmetry. Therefore, in order to observe this mode, one requires to perform a polarized INS measurement.

Based on the same reason, INS should see more resonances at Q_{11} and Q_{12} even in the non-polarized condition. However, the energy scale and intensity of those modes will depend at what location of the phase diagram of URu_2Si_2, the experiment is performed. As we argued earlier, Q_{11} is most likely responsible for the LMAF phase, therefore, we can expect a mode at twice of the corresponding gap opening. In the present work, we do not consider this phase and thus will be unable to predict its energy scale.

SELF-CONSISTENT GAP EQUATION

We can easily derive the self-consistent gap equation from Eq. 9 using Bogolyubov treatment. We substitute the fermion operator in terms of a hidden order quasiparticle state defined as $\gamma_{\boldsymbol{k},\tau\sigma} = u_{\boldsymbol{k}} f_{\boldsymbol{k},\tau\sigma} - v_{\boldsymbol{k}} f_{\boldsymbol{k}+\boldsymbol{Q},\tau\sigma}$ and replacing $\langle \gamma^\dagger_{\boldsymbol{k},\tau\sigma}\gamma_{\boldsymbol{k},\tau\sigma}\rangle = n^\nu_{f,\tau\sigma}(\boldsymbol{k})$. In doing so, we obtain the self-consistent gap equation as

$$\Delta^\mu_{\tau\tau'} = g_{0\tau\tau'} \sum_{\boldsymbol{k}} u_{\boldsymbol{k}} v_{\boldsymbol{k}} [1 - n^+_{f\tau\sigma}(\boldsymbol{k}) - n^-_{f\tau\sigma}(\boldsymbol{k})] \quad (16)$$

$$= \frac{1}{2} g_{0\tau\tau'} \sum_{\boldsymbol{k},\sigma} \frac{\Delta^\mu_{\tau\tau'}(\boldsymbol{k})}{E^{\tau\sigma}_{\boldsymbol{k}0}} [1 - n^+_{f\tau\sigma}(\boldsymbol{k}) - n^-_{f\tau\sigma}(\boldsymbol{k})] \quad (17)$$

We find that $g_{012} = 27$ meV gives $\Delta =$5 meV in consistent with experiments. For a temperature independent value of $g_{012} = 27$ meV, we obtain $T_h = 22$K, which is higher than the experimental value of $T_h = 17.5$ meV. Possible reasons for overestimating the value of T_h are the neglect of quantum fluctuation, disorder which can reduce its value. In this context, it can be noted that recently, a 'pseudogap' phase upto 20 K is marked from experimental features,[12] which arguably suggests that there are indeed fluctuations present above T_h.

QUANTUM CRITICAL POINT

As mentioned in the main text, any $\mathcal{TR}$ breaking perturbation such as magnetic field will destroy the $\mathcal{TR}$ invariant HO phase. As the HO state incipiently is a spontaneously broken symmetry, it exhibits a second order phase transition along the field axis. In what follows we expect to obtain a quantum critical point (QCP) at $T = 0$, as extensively proposed to be associated with any second order phase transition.[13] The experimental data[11] indicates that QCP resides around $B \sim 33$ T. The present model can not deduce the phase diagram for the superconducting (SC) state, possibly intervening the HO state, or any other phases that may arise above the QCP.[11]

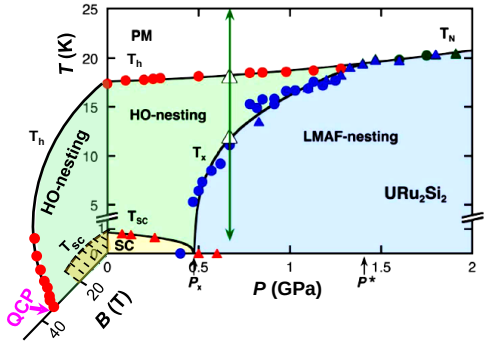

FIG. 3. Proposed phase diagram of URu_2Si_2 along the magnetic field ($\boldsymbol{B}$) direction. The data in pressure $(P)-T$ plane is taken from Ref. 10. The symbols in $B-T$ plane are extracted from Ref. 11. A QCP at $T=0$ along the field direction is expected from our theory, and also observed in experiment.[11] The phase diagram for SC and other possible phases that may arise above above the QCP is beyond the scope of the present calculation to deduce.

More experimental data and theoretical modeling are required to understand the details of this regime of the phase diagram.

[1] M. Dzero, K. Sun, K., V. Galitski, and P. Coleman, Phys. Rev. Lett. **104**, 106408 (2010).
[2] B. A. Bernevig, T. L Hughes, ans S.-C. Zhang, Science **314**, 1757 (2006).
[3] Xiao-Liang Qi, Taylor L. Hughes, and Shou-Cheng Zhang, Phys. Rev. B **78**, 195424 (2008).
[4] K. Haule, and G. Kotliar, Nat. Phys. **5**, 796-799 (2009).
[5] Dubi, Y., & Balatsky, A. V. Hybridization Wave as the Hidden Order in URu_2Si_2. *Phys. Rev. Lett.* **106**, 086401 (2011).
[6] P. Santini, Phys. Rev. B **57**, 5191-5199 (1998).
[7] E. Hassinger *et al.*, Phys. Rev. B **77**, 115117 (2008).
[8] Many-Particle Physics, Third Edition by G. Mahan. (Plenum).
[9] C. R. Wiebe *et al.*, Nat. Phys. **3**, 96 (2007).
[10] E. Hassinger *et al.*, Phys. Rev. B **77**, 115117 (2008)
[11] K. H. Kim *et al.*, Phys. Rev. Lett. **91**, 256401 (2003).
[12] J. T. Haraldsen, *et al.* Phys. Rev. B **84**, 214410 (2011).
[13] S. Sachdev, *Quantum Phase Transitions*, Cambridge University Press, Cambridge U.K. (1999).